Published OnlineFirst January 17, 2017; DOI: 10.1158/1078-0432.CCR-16-1464

Biology of Human Tumors

Clinical Cancer Research

In Hepatocellular Carcinoma miR-221 Modulates Sorafenib Resistance through Inhibition of Caspase-3–Mediated Apoptosis

Francesca Fornari[1,2], Daniela Pollutri[1], Clarissa Patrizi[3], Tiziana La Bella[4], Sara Marinelli[1], Andrea Casadei Gardini[5], Giorgia Marisi[6], Marco Baron Toaldo[7], Michele Baglioni[1], Veronica Salvatore[1], Elisa Callegari[8], Maurizio Baldassarre[1], Marzia Galassi[1], Catia Giovannini[1,2], Matteo Cescon[9], Matteo Ravaioli[9], Massimo Negrini[8], Luigi Bolondi[1,2], and Laura Gramantieri[1]

Abstract

Purpose: The aberrant expression of miR-221 is a hallmark of human cancers, including hepatocellular carcinoma (HCC), and its involvement in drug resistance, together with a proved *in vivo* efficacy of anti-miR-221 molecules, strengthen its role as an attractive target candidate in the oncologic field. The discovery of biomarkers predicting the response to treatments represents a clinical challenge in the personalized treatment era. This study aimed to investigate the possible role of miR-221 as a circulating biomarker in HCC patients undergoing sorafenib treatment as well as to evaluate its contribution to sorafenib resistance in advanced HCC.

Experimental Design: A chemically induced HCC rat model and a xenograft mouse model, together with HCC-derived cell lines were employed to analyze miR-221 modulation by Sorafenib treatment. Data from the functional analysis were validated in tissue samples from surgically resected HCCs. The variation of circulating miR-221 levels in relation to Sorafenib treatment were assayed in the animal models and in two independent cohorts of patients with advanced HCC.

Results: MiR-221 over-expression was associated with Sorafenib resistance in two HCC animal models and caspase-3 was identified as its target gene, driving miR-221 anti-apoptotic activity following Sorafenib administration. Lower pre-treatment miR-221 serum levels were found in patients subsequently experiencing response to Sorafenib and an increase of circulating miR-221 at the two months assessment was observed in responder patients.

Conclusions: MiR-221 might represent a candidate biomarker of likelihood of response to Sorafenib in HCC patients to be tested in future studies. Caspase-3 modulation by miR-221 participates to Sorafenib resistance. *Clin Cancer Res; 23(14); 3953–65. ©2017 AACR.*

Introduction

The up-regulation of miR-221 along with its oncogenic activity were previously reported in hepatocellular carcinoma (HCC; refs. 1–3), as well as in other cancers, such as glioblastoma (4, 5), papillary thyroid carcinoma (6, 7), pancreatic cancer (8), prostate (9), melanoma (10), breast (11), kidney, and bladder cancers (12). Onco-miR-221 upregulation can be considered a hallmark of cancer. We have also shown its tumor-promoting functions in the liver of a miR-221 transgenic mouse, confirming its role as a therapeutic candidate (13).

Molecular mechanisms sustaining miR-221 oncogenic functions rely upon the regulation of cell proliferation (1) and impairment of apoptosis (3, 5). In addition, miR-221 plays an important role in the modulation of response to anticancer treatments through the regulation of key oncogenic factors such as the *TP53–MDM2* axis (14), *TIMP3* (15), and *PTEN* (16) molecules.

Even though sorafenib represents the standard of care for advanced HCC and it is the only recommended treatment in this setting, there is no biomarker helpful in the prediction of sensitivity to this treatment. However, heterogeneous responses may be observed across patients treated by sorafenib.

The discovery of novel target candidates increasing the efficacy of anticancer strategies and the identification of noninvasive biomarkers in liquid biopsies are two important clinical challenges in the oncologic field. It was widely demonstrated that microRNAs are optimal biomarkers due to their high stability in biologic fluids and the availability of easy detection methods (17, 18).

[1]Center for Applied Biomedical Research, St.Orsola-Malpighi University Hospital, Bologna, Italy. [2]Department of Medical and Surgical Sciences, Bologna University, Bologna, Italy. [3]Center for Regenerative Medicine, Department of Biomedical Sciences, University of Modena and Reggio Emilia, Modena, Italy. [4]INSERM, UMR-1162, Functional Genomics of Solid Tumors, Paris, France. [5]Department of Medical Oncology, Istituto Scientifico Romagnolo per lo Studio e la Cura dei Tumori (IRST) IRCCS, Meldola, Italy. [6]Biosciences Laboratory, Istituto Scientifico Romagnolo per lo Studio e la Cura dei Tumori (IRST) IRCCS, Meldola, Italy. [7]Department of Veterinary Medical Sciences, Bologna University, Bologna, Italy. [8]Department of Morphology, Surgery and Experimental Medicine, Ferrara University, Ferrara, Italy. [9]Department of Medical and Surgical Sciences, General and Transplant Surgery Unit, St. Orsola-Malpighi University Hospital, Bologna, Italy.

Note: Supplementary data for this article are available at Clinical Cancer Research Online (http://clincancerres.aacrjournals.org/).

D. Pollutri, C. Patrizi, T. La Bella contributed equally to this article.

Corresponding Authors: Francesca Fornari, Via Massarenti, 9, 40138, Bologna, Italy. Phone/Fax: 390512143902; E-mail: francesca.fornari2@unibo.it; and Laura Gramantieri, laura.gramantieri@aosp.bo.it

doi: 10.1158/1078-0432.CCR-16-1464

Published OnlineFirst January 17, 2017; DOI: 10.1158/1078-0432.CCR-16-1464

Here, we explored, by using an *in vivo* and *in vitro* approach, the role of miR-221 as a tissue and circulating biomarker in the setting of sorafenib treatment. To this aim, we used two HCC models, a diethylnitrosamine (DEN)-induced HCC rat model and a xenograft mouse model, as well several HCC-derived cell lines. Moreover, we tested the circulating levels of miR-221 as a candidate noninvasive biomarker associated with response to sorafenib treatment in advanced HCC, both in animal models and in a small and preliminary cohort of HCC patients. Finally, molecular mechanisms sustaining the role of miR-221 as an innovative therapeutic target in HCC were investigated, and caspase-3 modulation was assessed as a critical factor.

Patients and Methods

Patients

HCC and cirrhotic tissues were obtained from 60 randomly selected patients (45 males and 15 females, median age ± SD, 70.0 ± 8.5 years; range, 49–82 years) undergoing liver resection for HCC. Tissues were collected at surgery and stored as previously described (19). Local ethics committee of St. Orsola-Malpighi University Hospital approved the study, and all patients signed an informed consent. Histopathologic grading was scored according to Edmondson and Steiner criteria (20). No patient received anticancer treatment prior to surgery. Antiviral treatment was administered to HBV-infected patients only. No HCV-infected patient received antiviral treatment except for interferon-based regimens performed at least 3 years before surgery. Eight normal liver tissues were obtained from patients undergoing liver surgery for traumatic lesions (5 cases) or hemangioma resection (3 cases). The characteristics of patients are detailed in Supplementary Table S1.

A further cohort of 93 patients with advanced HCC without extrahepatic metastases were tested for miR-221 circulating levels. Fifty patients from Bologna center (23 responders and 27 nonresponders at 2 months) were tested before treatment start. Among these, 28 patients (12 responders and 16 nonresponders) were assayed before treatment and at the 2 months assessment. The remaining 43 patients (17 with stable disease and 26 patients with disease progression at 2 months) were tested for circulating miR-221 levels before treatment start (43 cases) and at the 2 months assessment (31 of 43 patients). These 43 patients were enrolled by both the Bologna Center and the Department of Medical Oncology of Meldola's Center (Italy) and were considered as an independent validation cohort. Patients' characteristics are detailed in Supplementary Table S2 and Supplementary Fig. S1.

DEN-HCC rat model

Male Wistar rats (Harlan) received DEN (Sigma-Aldrich) in the drinking water (100 mg/L) for 8 weeks. Two weeks later the end of DEN treatment, animals were weekly monitored by ultrasound imaging (US; MyLab70 XVG, Esaote; ref. 21). A first group of animals ($N = 18$) was euthanized 1 or 2 months after the end of DEN treatment, when the major diameter of at least one HCC nodule reached a dimension of 10 mm at US. A second group of animals ($N = 10$) received sorafenib intragastrically for 21 days (10 mg/kg of body weight), starting when a 2- to 3-mm nodule was evident at US. Animals were segregated in responder and nonresponder groups according to US and histopatologic examination. Two untreated animals were used as control. At sacrifice, HCC nodules and surrounding liver were collected for molecular biology and immunohistochemistry analyses. Twenty-three and 16 HCC nodules were collected in the untreated and treated groups, respectively. At sacrifice, blood withdrawal was obtained from 13 of 18 untreated and 7 of 10 sorafenib treated rats. Serum was achieved by centrifugation of blood samples at 4,000 rpm for 10 minutes at 4°C. All animals received human care in accordance with the criteria published by the National Institutes of Health. Local ethics committee approved the research protocol (14/70/12).

HCC mice models

For the xenograft model, 3.0 million of Huh-7 cells were injected into both flanks of NOD/SCID (CB17PRKDC/J) female mice ($N = 15$ animals). Four weeks following cell injection, tumor masses were weekly monitored by US examination, and when the tumors reached a volume of about 40 to 50 mm^3 (width × length × height/2) mice were randomized into two groups. One group ($N = 6$) received intragastrically a dose of 60 mg/kg body weight of sorafenib for 21 days, while the other group ($N = 9$) received only the vehicle (75% water, 12.5% absolute ethanol, and 12.5% cremophor EL; Sigma-Aldrich). Mice were euthanized one day after the end of the treatment or, in the case of the untreated group, when the tumor mass exceeded the volume of about 1 cm^3. At sacrifice, tumor masses were collected for both molecular biology and histopathology analyses. At sacrifice, blood withdrawal was obtained from all mice of the vehicle-treated group and from 5 of 6 sorafenib-treated animals. Serum samples were obtained as above described. Local ethics committee approved the research protocol (23/79/14).

The miR-221 transgenic mouse model was performed as previously described (13, 14). Protein samples were extracted from liver tissues derived from 25 transgenic (TG) and 16 wild-type (WT) animals. Ten TG mice were treated by hydrodynamic tail vein injection with anti-miR-221 oligonucleotides (300 μg/mouse) or with vehicle only (saline) for 48 hours. Four more animals were treated with anti-miR-221 oligonucleotides or with vehicle only in the presence of sorafenib treatment (intragastrical administration, 10 mg/kg) for 48 hours.

Cell culture and treatments

HepG2, Hep3B, and PLC/PRF/5 cells were cultured with Eagles's Minimum Essential Medium while SNU398, SNU449, SNU182, SNU475, and Huh-7 were cultured with RPMI-1640 (Life Technologies). Media were supplemented with 10% FBS, 2 mmol/L L-glutamine and 1× penicillin/streptomycin (Life Technologies). All the cell lines, except Huh-7, were purchased from ATCC. Huh-7 cells are from Prof. Alberti's laboratory, University of Padua, Italy. Cell clones used for experiments were previously authenticated. Cells were treated with 5.0 μmol/L sorafenib-tosylate (Bayer) for 48 hours. All experiments were performed in triplicate.

Cells were also treated with 1.0 μmol/L of PI3Kα/δ inhibitor (GDC-0941), Raf inhibitor (PLX-4720), and VEGFR2 inhibitor (ZM323881) for 48 hours (Selleckchem).

Cell transfection

HCC cells were transfected with 100 nmol/L of pre-miR-221, anti-miR-221, or Negative Control#1 precursor and inhibitor miRNAs (Ambion). BMF and caspase-3 small interfering RNA pools (Trifecta RNAi Kit, IDT) were used at a concentration of 20 nmol/L for 24 and 48 hours. Oligonucleotide transfection was

Published OnlineFirst January 17, 2017; DOI: 10.1158/1078-0432.CCR-16-1464

performed by using Lipofectamine 2000 (Life Technologies) according to the manufacturer's instructions.

Stable transfection

For miR-221 overexpression in Huh-7 cells, the DNA sequence of mature miR-221 was inserted into the pGFP-V-RS retroviral vector (OriGene Technologies). The cells were infected and selected as previously described (14).

Luciferase activity assay

The 3′UTR region of human CASP3 gene was amplified by PCR using primers and conditions reported in Supplementary Table S3. A luciferase reporter assay of pGL3 3′UTR-containing vector was performed in HepG2 and SNU449 cells as previously reported (22).

Caspase 3/7 activity assay and viability assay

Apoptosis activation and cell viability were evaluated in sorafenib-treated HCC cells by using Caspase-Glo 3/7 and Cell-titer-Glo assays (Promega) according to the manufacturer's instructions. Each sample was analyzed in quadruplicate.

Real-time PCR and RT-PCR

MiRNA-221-3p expression in HCC cells and tissue samples was evaluated by the TaqMan MicroRNA Assay (ID: 000524; Applied Biosystems), as previously described (19). RNU6B (ID: 001093) was used as housekeeping gene for human samples, whereas 4.5S RNA(H) (ID: 001717) and snoRNA412 (ID: 001243) were used for samples of rat and mouse origin, respectively. A pool of RNAs from two HCC cell lines or two HCC rat livers or two mouse livers was used as reference sample for the $2^{-\Delta\Delta Ct}$ method for the quantification of samples of human or rat or mouse origin, respectively.

CASP3, *BMF*, *AFP*, *EpCAM*, *CK19*, and *MYC* mRNAs were quantified by both semi-quantitative PCR and SYBR-green (Bio-Rad Laboratories) Real-time PCR analyses. β-Actin expression was considered for gene normalization. Real-time PCR experiments were run in triplicate. Primers and conditions are detailed in Supplementary Table S4.

Serum and exosome miRNA extraction

Isolation of circulating miRNAs from exosomes and cell culture supernatant of untreated and sorafenib-treated HCC cells was executed by an ultracentrifugation-based protocol as previously reported (23). Total RNA was isolated from 200 μL of serum, cell culture supernatant, exosomes enriched or depleted fractions by using MiRNeasy Serum/Plasma Kit (Qiagen). Briefly, 12.5 fmol of a synthetic RNA corresponding to cel-miR-39 sequence (Ambion) were added to each sample after Qiazol addition. RNA was suspended in 35 μL of DEPC water and used at a 1:3 dilution for qPCR quantification of miR-221 and cel-miR-39.

Western blot

Thirty micrograms of whole protein extracts from cells and tissues was subjected to vertical electrophoresis, transferred to a nitrocellulose membrane (GE Healthcare) and assayed with antibodies reported in Supplementary Table S5. Digital images of X-ray films were quantified by ChemiDoc XRS+ (Image Lab Software, Bio-Rad). Western blot analysis was performed in triplicate.

Flow cytometry analysis

Transfected HCC cells were treated with 5 μmol/L sorafenib for 48 hours. Detection of apoptotic cells was performed in triplicate by flow cytometry (FACSaria cell sorter, BD Biosciences) with Annexin V/Propidium Iodide detectionkit (Bender MedSystems).

Statistical analysis

Differences between groups were analyzed using paired or unpaired Student *t* test, for *in vitro* assays and for the analysis of HCC-related variables, including miR-221 and caspase-3 expression in primary tumors as well as circulating miR-221 levels. Pearson correlation coefficient was used to explore relationships between two variables. *In vitro* experiments were performed in triplicate, and the mean values were used for the statistical analysis. Reported *P* values were two-sided and considered statistically significant when lower than 0.05. Statistical calculations were executed using SPSS version 15.0 (SPSS inc). *, $P < 0.05$; **, $P < 0.01$; ***, $P < 0.001$.

Results

High intratumor miR-221 levels are associated with sorafenib resistance in HCC animal models

The role of onco-miR-221 in hepatocarcinogenesis (13, 19, 24) and response to treatments in HCC is documented (14–16). Here, we used two HCC animal models to investigate miR-221 involvement in sorafenib resistance.

The first animal model is a chemically induced HCC rat model displaying miR-221 overexpression in tumor tissue in 65% of cases, with a mean increase of 2.8-fold in HCC nodules ($N = 23$) when compared with matched surrounding liver ($N = 16$; Fig. 1A). Notably, miR-221-deregulated expression observed in this model reflects findings reported in human HCC (19). Moreover, the nonneoplastic liver tissue of DEN-treated animals displays no difference in miR-221 expression when compared with healthy control rats, ruling out miR-221 modulation by DEN.

Following sorafenib administration, HCC nodules ($N = 16$) were considered as responders or nonresponders, based on US monitoring performed weekly during the follow-up after DEN discontinuation and histopathologic examination at sacrifice (Supplementary Fig. S2). QPCR analysis showed higher intratumor miR-221 levels in nonresponder versus responder rat HCCs (Student *t* test: $P = 0.0013$; Fig. 1B), suggesting that miR-221 might be implicated in sorafenib resistance. To characterize if sorafenib resistance might be related to the expression of specific oncogenes, *AFP*, *EPCAM*, *CK19*, and *MYC* mRNA levels were analyzed in treated HCC animals. Higher *EPCAM* mRNA were detected in HCC nodules non-responding to sorafenib with respect to the responder group (Student *t* test: $P = 0.0011$; Fig. 1C), while no difference was detected for *AFP*, *CK19*, and *MYC* expression (Supplementary Fig. S3A–S3C).

The second animal model was a xenograft mouse model obtained by subcutaneous injection of Huh-7 cells into animal flanks. This model was chosen because it displays a relevant response to sorafenib treatment, which is easily assessable by US examination (25). In this model, sorafenib administration determined a reduction of tumor size of 3.5-fold with respect to vehicle-treated mice (mean ± SD: 238 ± 119 vs. 836 ± 490 mm^3; Student *t* test: $P = 0.0062$; Fig. 1D). Similarly, a 1.6-fold increase in tumor doubling time was observed in sorafenib-treated mice in comparison with controls (mean ± SD: 4.3 ± 2.0 vs. 6.9 ± 0.9 mm^3; Student *t* test, $P = 0.0044$; Fig. 1E). An inverse correlation

Published OnlineFirst January 17, 2017; DOI: 10.1158/1078-0432.CCR-16-1464

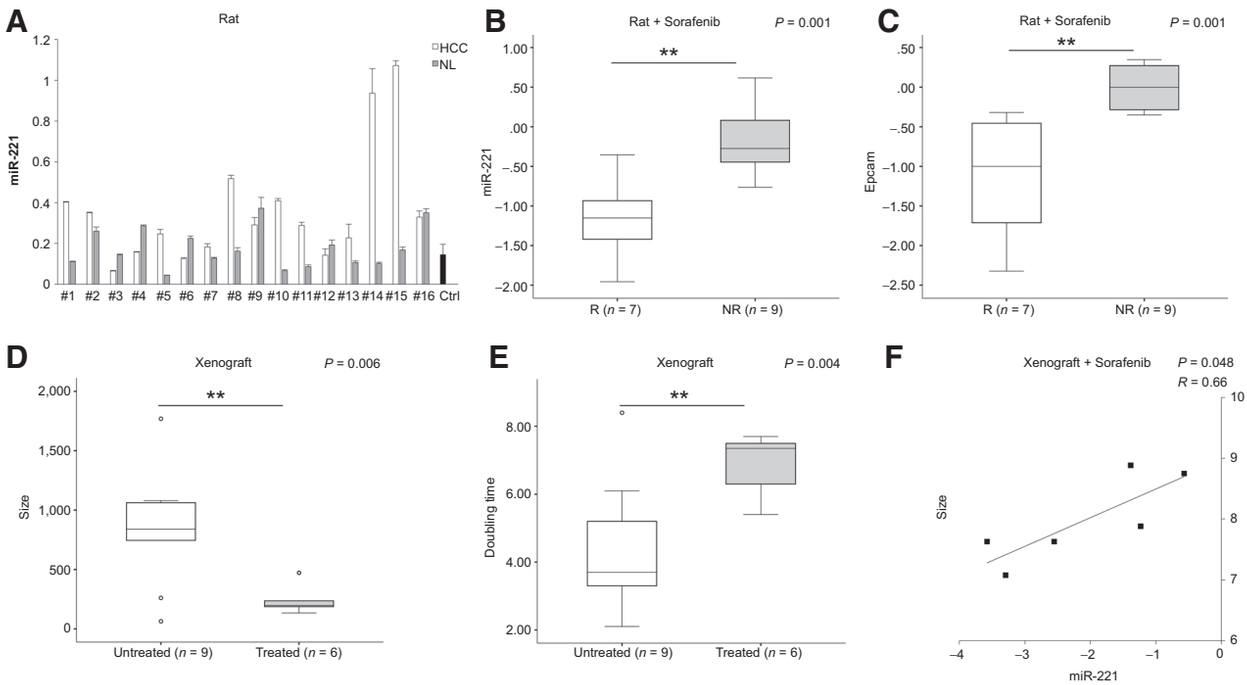

Figure 1.

MiR-221 correlates with sorafenib resistance in HCC animal models. **A,** qPCR analysis of miR-221 expression in 16 DEN-treated rats and two healthy controls (Ctrl). Each nodule was compared with the surrounding liver parenchyma (NL). The y-axis reports the $2^{-\Delta\Delta Ct}$ values corresponding to miR-221 expression. **B and C,** Box plot graphic representation of miR-221 and *EPCAM* mRNA expression in DEN-treated rats following 21 days of sorafenib administration ("rat + sorafenib"). HCC nodules were divided in responders (R) and nonresponders (NR) based on US imaging and histopathologic examination. The y-axis reports the $2^{-\Delta\Delta Ct}$ values corresponding to gene expression (log_2 form). **D and E,** Box plot graphic representation of tumor size or tumor doubling time in sorafenib-treated or untreated xenograft mice obtained following subcutaneous injection of Huh-7 cells into the flank of nude mice ("xenograft"). The treated group received sorafenib intragastrically for 21 days; the untreated group received only the vehicle. The y-axis represents tumor size (mm^3) or tumor doubling time (days). **F,** Correlation graph between tumor size and miR-221 expression in sorafenib-treated xenograft mice. The xenograft model was obtained by subcutaneous injection of Huh-7 cells, and once the tumors reached a volume of 40–50 mm^3, mice received sorafenib intragastrically for 21 days ("xenograft + sorafenib"). The *x*-axis reports the $2^{-\Delta\Delta Ct}$ values corresponding to miR-221; y-axis represents tumor size (mm^3). All values are transformed in a log_2 form.

was found between tumor size and tumor doubling time (Pearson correlation, $P = 0.002$; Supplementary Fig. S3D).

When miR-221 levels were assessed in the tumor masses from untreated animals, no correlation was found with respect to size and tumor doubling time. Conversely, in sorafenib-treated mice a positive correlation was detected between miR-221 expression and tumor size (Pearson correlation: R = 0.66; $P = 0.048$; Fig. 1F), letting us to hypothesize that also in this model high miR-221 levels might be associated with sorafenib resistance.

Circulating miR-221 levels predict response to sorafenib

Because higher miR-221 tissue levels are associated with sorafenib resistance in the rat HCC model and with increased tumor mass in the xenograft model, we investigated the relationships between tissue and circulating miR-221 levels in these models, to define its role as a possible circulating biomarker.

MiR-221 expression was quantified in serum samples and tumor tissues from 13 DEN-HCC–untreated rats. As shown in Fig. 2A, a correlation was found between miR-221 levels in HCC tissue and serum samples (Pearson correlation: R = 0.58; $P = 0.045$). Only the larger nodule was considered in animals bearing more than one HCC, hypothesizing that it might be the main source of miRNAs release into the bloodstream. When considering more nodules in rats with a multinodular HCC, a positive correlation, even though not statistically significant, was confirmed between tissue and circulating miR-221 levels (Pearson correlation: R = 0.42; $P = 0.087$; Supplementary Fig. S3E).

These findings were confirmed in the mouse model displaying a correlation between circulating and intratumor miR-221 levels in untreated animals (Pearson correlation: R = 0.66; $P = 0.048$; Fig. 2B).

Subsequently, we tested circulating miR-221 levels in the setting of sorafenib treatment in both models. Sorafenib treated DEN-HCC rats displayed an inverse correlation between circulating and tissue miR-221 levels (Pearson correlation: R = −0.75; $P = 0.050$; Fig. 2C). This finding suggests that sorafenib might have a role in miR-221 release from neoplastic hepatocytes into the bloodstream. The same result was confirmed in the mouse model, displaying a negative correlation between circulating miR-221 levels and both tissue miR-221 levels (Pearson correlation: R = −0.88; $P = 0.047$) and tumor size (Pearson correlation: R = −0.96; $P = 0.003$; Fig. 2D and E).

We next explored the mechanisms contributing to miR-221 release into the bloodstream in basal conditions as well as

Published OnlineFirst January 17, 2017; DOI: 10.1158/1078-0432.CCR-16-1464

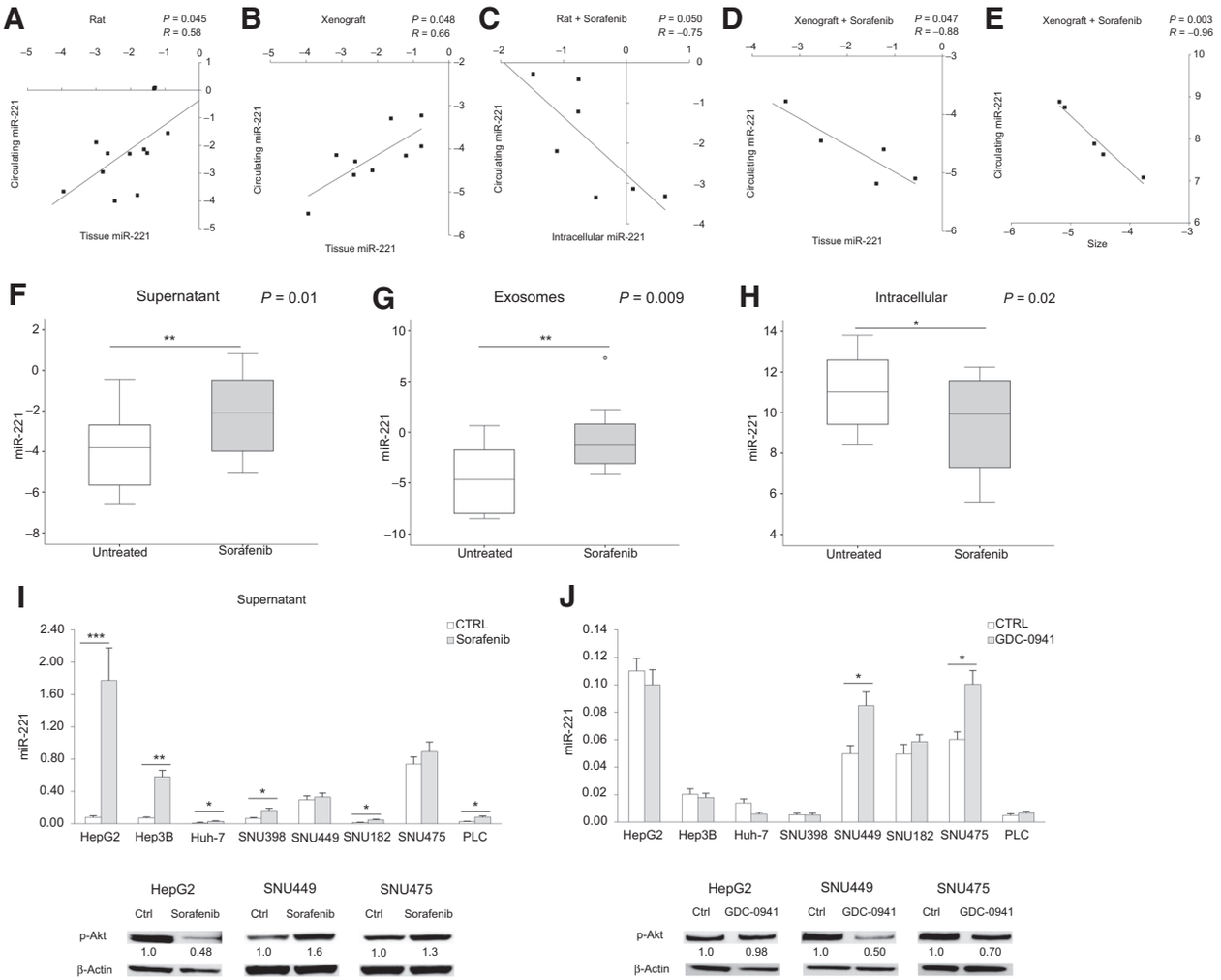

Figure 2.

Circulating miR-221 levels in HCC animal models treated with sorafenib. **A,** Correlation between extracellular and intracellular miR-221 levels in the DEN-HCC rat model ($N = 13$). X and Y-axes report the $2^{-\Delta\Delta Ct}$ values corresponding to intratumor and circulating miR-221 levels. **B,** Correlation between extracellular and intracellular miR-221 levels in the xenograft model ($N = 9$). X and Y-axes report the $2^{-\Delta\Delta Ct}$ values corresponding to intratumor and circulating miR-221 levels. **C,** Negative correlation between extracellular and intracellular miR-221 levels in the DEN-HCC rat model treated by sorafenib ($N = 7$). X and Y-axes report the $2^{-\Delta\Delta Ct}$ values corresponding to intratumor and circulating miR-221 levels. **D** and **E,** Negative correlation between extracellular and intracellular miR-221 levels or tumor size in sorafenib-treated xenograft model ($N = 5$). X-axes report the $2^{-\Delta\Delta Ct}$ values corresponding to miR-221 intra-tumor levels or tumor size (mm^3), respectively. Y-axes report the $2^{-\Delta\Delta Ct}$ values corresponding to circulating miR-221 levels. **F–H,** Box plot graph of miR-221 expression in cell culture supernatant, exosomal, and intracellular fractions of sorafenib-treated and untreated cell lines. Y-axes report the $2^{-\Delta\Delta Ct}$ values corresponding to miR-221 expression. **A–H,** All values are transformed in a $\log_2$ form. **I,** Circulating miR-221 levels in cell culture supernatant of HCC cells treated with sorafenib or vehicle (Ctrl) for 48 hours. **J,** Circulating miR-221 levels in cell culture supernatant of HCC cells treated with PI3K inhibitor (GDC-0941) or vehicle (Ctrl) for 48 hours. **I** and **J,** Y-axes report the $2^{-\Delta\Delta Ct}$ values corresponding to miR-221 expression. Cel-miR-39 was used to normalize QPCR data. Western blot analysis of pAkt in HepG2, SNU449 and SNU475 in the same settings. β-Actin was used to normalize WB data. *, $P < 0.05$; **, $P < 0.01$; ***, $P < 0.001$.

following sorafenib. Eight HCC-derived cell lines were assayed, and a correlation between miR-221 levels in cell culture supernatant and exosome fraction was found, suggesting exosome vesicles as a source of circulating miR-221 (Pearson correlation: $R = 0.928$; $P = 0.001$), as previously demonstrated by us in HCC patients (23).

In HCC cells, sorafenib increased miR-221 levels in cell culture supernatant (Student *t* test: $P = 0.01$; Fig. 2F), as well as in its exosomal fraction (Student *t* test: $P = 0.009$; Fig. 2G), while miR-221 levels decreased in the intracellular compartment (Student *t* test: $P = 0.02$; Fig. 2H). These findings suggest a direct role of sorafenib in the variation of miR-221 expression in both the intracellular and extracellular compartments in HCC. To evaluate which molecular pathway modulated by sorafenib was mainly involved in miR-221 secretion from the intra to the extracellular compartment, we tested eight HCC-derived cell lines with three inhibitors of molecular pathways modulated by sorafenib (PLX-4720 inhibiting *BRAF*, *RAF1*, and *CRAF*; ZM323881 inhibiting *VEGFR2*; GDC-0941 inhibiting *PI3Kα/δ*). We compared miR-221 changes in the

Published OnlineFirst January 17, 2017; DOI: 10.1158/1078-0432.CCR-16-1464

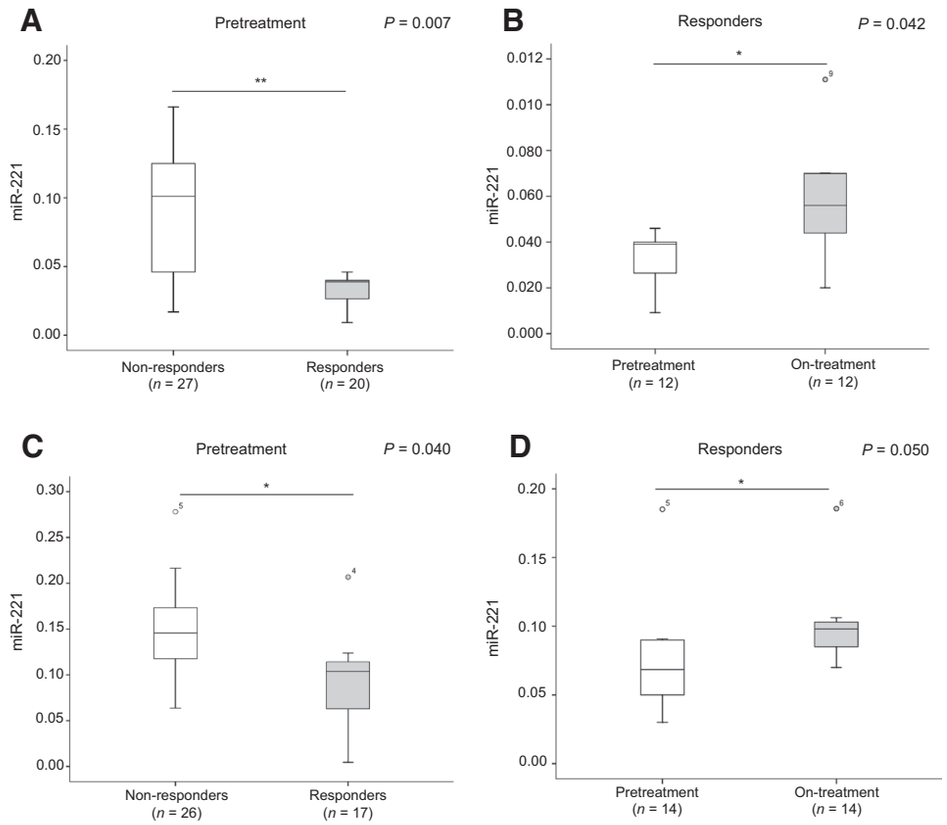

Figure 3.
Circulating miR-221 in patients with advanced HCC treated with sorafenib. **A,** Basal miR-221 levels in patients responding or nonresponding to sorafenib treatment, as assessed at the two months CT/MR examination, in the training set. **B,** Circulating miR-221 levels assessed before sorafenib start and at the two months follow-up in patients responding to sorafenib in the training set. **C,** Circulating miR-221 levels in patients responding or non-responding to sorafenib, as assessed at the 2 months CT/MR examination, in the validation set. **D,** Circulating miR-221 levels assessed before sorafenib start and at the 2 months follow-up in patients responding to sorafenib in the validation set. **A** and **C,** Unpaired Student *t* test was considered for statistical analysis. **B** and **D,** Paired Student *t* test was considered for statistical analysis. **A–D,** RNU6B was used as housekeeping gene for QPCR analysis. Y-axes report $2^{-\Delta\Delta Ct}$ values corresponding to circulating miR-221 levels. Pretreatment: circulating miR-221 levels were evaluated in sera samples collected before treatment. On-treatment: circulating miR-221 levels were evaluated in sera samples collected at 2 months CT/MR assessment.

extracellular compartments in treated versus untreated cells. PLX-4720 administration, inhibiting the Ras/Raf/Mek/Erk pathway, determined an increase in miR-221 extracellular levels in SNU475 cells only, while no relevant increase was detected in the other cell lines. Similarly, no significant increase was observed following VEGFR2 inhibition, obtained by ZM323881 administration, in all the cell lines. The inhibition of PI3Kα/δ was performed due to the relevant role of pAKT in exosomal trafficking in cancer cells. Because a high heterogeneity was found in constitutive activation of the MAPK and PI3K–Akt pathways, HCC-derived cell lines were evaluated taking into account basal expression levels of each pathway and the extent of miR-221 variations following treatments. Sorafenib administration determined miR-221 extrusion from the intra to the extracellular compartment in HepG2 (with the most relevant effect), Hep3B, Huh-7, SNU398, SNU182, and PLC cells, but not in SNU475 and SNU449 cells. Notably, following sorafenib treatment, an opposite phosphorylation pattern of Akt was observed in HepG2 versus SNU449 and SNU475 cells. Therefore, we hypothesized that pAkt levels might be relevant as far as miR-221 release from HCC cells is concerned (Fig. 2I). A relevant increase of miR-221 extracellular levels was observed by PI3K inhibition in SNU449 and SNU475 cells. The effects on miR-221 extrusion in HepG2, SNU449, and SNU475 cells treated by sorafenib was thus opposite to what observed following GDC-0941. GDC-0941 treatment was not able to reduce pAkt levels in HepG2 cells where no variation of miR-221 extracellular levels was detected, whereas it reduced pAkt levels in SNU449 and SNU475 cells where an increase of miR-221 extrusion was detected (Fig. 2J). Thus, we can speculate that the inhibition of the PI3K–pAkt axis by GCD-0941 might be responsible for miR-221 extrusion in these cells. Notably, the extent of sorafenib treatment in miR-221 secretion is higher than that observed after PI3K inhibition, thus supporting the contribution of other molecular events.

High circulating miR-221 levels are associated with response to sorafenib in HCC patients.

As described above, both rodent models suggested that higher miR-221 tissue levels were associated with sorafenib resistance. Conversely, higher circulating miR-221 levels correlated with smaller tumor size and inversely correlated with tissue miRNA levels. These findings prompted us to assay circulating miR-221 levels in sorafenib-treated HCC patients.

To test miR-221 as a possible circulating biomarker predicting the likelihood of response to sorafenib, we analyzed miR-221 levels in sera from HCC patients before sorafenib treatment. Patients experiencing radiologic disease progression ($N = 27$) showed higher pretreatment miR-221 levels when compared with responders ($N = 23$), as assessed at 2 months CT/MR examination (*t* test: $P = 0.007$; Fig. 3A). Among the 50 patients tested before treatment start, 28 patients (12 responders and 16 nonresponders) were further tested at 2 months follow-up. When comparing pretreatment and on-treatment miR-221 levels in the same patient, an increase of miR-221 levels was detected in responders (paired *t* test: $P = 0.042$; Fig. 3B), whereas a nonsignificant decrease of miR-221 levels was registered in nonresponders (paired *t* test: $P = 0.058$).

Published OnlineFirst January 17, 2017; DOI: 10.1158/1078-0432.CCR-16-1464

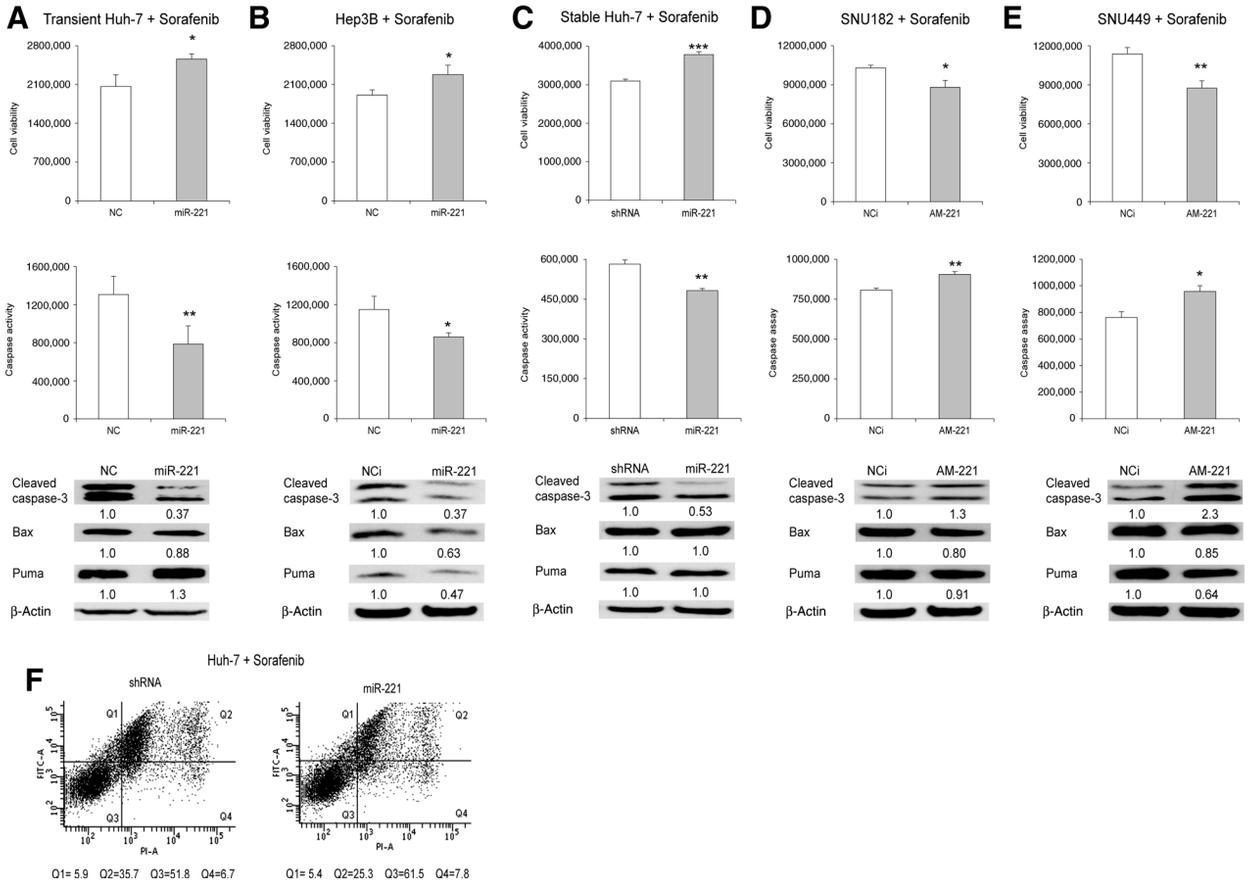

Figure 4.

MiR-221 decreases sorafenib activity in HCC cell lines. **A** and **B,** Cell viability assay, caspase 3/7 activity assay, and Western blot analysis in transient miR-221 overexpressing Huh-7 and Hep3B cells subjected to sorafenib. **C,** Cell viability assay, caspase 3/7 activity assay, and Western blot analysis in Huh-7 cells stably infected with pMXs-miR-221 overexpression vector subjected to sorafenib treatment. **D** and **E,** Cell viability assay, caspase 3/7 activity assay, and Western blot analysis in transient miR-221 silenced SNU182 and SNU449 cells following sorafenib treatment. **F,** Annexin V cytofluorimetric analysis in miR-221 stably overexpressing Huh-7 cells subjected to sorafenib treatment. **A–F,** NC: pre-miR–negative control; NCi: anti-miR–negative control; AM-221: anti-miR-221; shRNA: scramble short hairpin RNA control vector. **A–E,** β-actin was used to normalize WB data.

An independent small validation cohort of 43 advanced HCC patients enrolled by the Department of Medical Oncology of the Meldola's Cancer Center and by the Bologna's Center was assessed for circulating miR-221 before treatment start and at the 2 months follow-up in 31 of 43 patients. Even though the number of patients included is too small to draw any conclusion, this validation series confirmed the findings obtained in the training set, as shown in Fig. 3C. The 26 patients experiencing a partial response or disease progression at 2 months displayed higher miR-221 serum levels when compared with the 17 patients with a stable disease (t test, $P = 0.04$). Among the 17 responders, 14 patients were assessed also at the 2 months follow-up, and an increase of miR-221 circulating levels was confirmed when compared with miR-221 pretreatment levels (paired t test, $P = 0.05$). As observed in the training set, a nonsignificant reduction of miR-221 serum levels at the 2 months follow-up was observed in 17 of 26 tested nonresponder patients (paired t test, $P = 0.07$). In conclusion, lower pretreatment miR-221 serum levels are associated with response to sorafenib. In addition, treatment response was associated with an increase of circulating miR-221, suggesting a possible secretion of this onco-miRNA from the intracellular compartment of neoplastic cells.

MiR-221 decreases apoptosis in sorafenib-treated HCC cell lines

To study miR-221 involvement as a possible contributor to sorafenib resistance, HCC-derived cells were transfected with pre- or anti-miR-221 and treated with sorafenib for 48 hours.

Specifically, we chose Huh-7 and Hep3B cells for miR-221 overexpression because of their low miR-221 basal levels, while miR-221 silencing was performed in SNU449 and SNU182 cells due to their high miR-221 basal levels, as previously reported (14). Transient miR-221 overexpression in sorafenib-treated Huh-7 and Hep3B cells increased cell viability (Student t test: $P = 0.04$ and $P = 0.017$, respectively) and decreased caspase 3/7 activity (Student t test: $P = 0.006$ and $P = 0.033$, respectively) and expression (Fig. 4A and B). A similar effect was observed in Huh-7 cells stably overexpressing miR-221, indicating that even a low miR-221 increase (6.5-fold) is sufficient to reduce sorafenib

Published OnlineFirst January 17, 2017; DOI: 10.1158/1078-0432.CCR-16-1464

anticancer activity (Student *t* test: $P = 0.0008$ and $P = 0.002$ for cell viability and caspase assay, respectively; Fig. 4C). Conversely, miR-221 silencing in sorafenib-treated SNU182 and SNU449 cells decreased cell viability (Student *t* test: $P = 0.03$ and 0.001, respectively) and increased caspase 3/7 activity (Student *t* test: $P = 0.003$ and 0.016, respectively) and expression (Fig. 4D and E). Notably, miR-221 did not alter Bax and Puma protein expression in all the cell lines except Hep3B (Fig. 4A–E), suggesting a main involvement of the caspase cascade in miR-221–mediated sorafenib resistance. FACS–Annexin V assay performed in stably overexpressing miR-221 Huh-7 cells following sorafenib challenge further confirmed these data. A 1.4-fold decrease of events in late apoptosis was detected in miR-221 overexpressing cells (Student *t* test: $P = 0.01$; Fig. 4F). These data highlighted an involvement of miR-221 in sorafenib resistance of HCC cells, associated with inhibition of the caspase signaling.

MiR-221 targets caspase-3 in HCC cell lines

To clarify mechanisms sustaining miR-221 involvement in sorafenib resistance, a computational analysis was performed identifying *CASP3* (NM_004346) among its target genes (TargetScan and MiRanda algorithms; Fig. 5A). To identify the best *in vitro* models to study caspase-3 regulation by miR-221, their expression levels were assayed in HCC-derived cell lines. An inverse correlation was found between miR-221 and caspase-3 mRNA and protein levels (Spearman correlation $P = 0.036$; Fig. 5B).

The functional analysis was performed based on miR-221 basal levels in HCC cells. HepG2 and Huh-7 cells were chosen for miR-221 overexpression, whereas SNU449 and SNU182 cells were selected for miR-221 silencing. Cell transfection of pre-miR-221 in HepG2 and Huh-7 cells reduced caspase-3 expression at both protein and mRNA levels. The same was confirmed in Huh-7 cells stably overexpressing miR-221, by retroviral infection (Fig. 5C–E). Conversely, anti-miR-221 transfection in SNU449 and SNU182 cells increased both caspase-3 mRNA and protein expression (Fig. 5F and G). To prove a direct interaction between miR-221 and its target gene, the 3′UTR region of caspase-3 mRNA was cloned downstream a reporter gene and the resulting vector (pGL3-casp-3) was employed in a dual-luciferase assay. Cotransfection of pGL3-casp-3 vector with miR-221 in HepG2 cells or with AM-221 in SNU449 cells caused a 1.5-fold decrease and a 1.6-fold increase of the luciferase activity, respectively (Student t-test: $P = 0.007$ and $P = 0.001$, respectively; Fig. 5H). Finally, to demonstrate that caspase-3 targeting is an important mechanism mediating sorafenib resistance by miR-221, SNU449 cells were cotransfected with anti-miR-221 oligonucleotides and caspase-3 siRNAs and subsequently treated with sorafenib. WB analysis showed that caspase-3 inhibition was able to counteract the activation of the caspase cascade triggered by miR-221 silencing, decreasing the levels of cleaved fractions of caspase-3, caspase-7, and PARP, with respect to anti-miR-221–only transfected cells (Fig. 5I). These data demonstrated that miR-221 directly modulates caspase-3 expression in HCC cells by mRNA degradation and that caspase-3 targeting is involved, at least in part, in miR-221–mediated sorafenib resistance.

MiR-221 regulates caspase-3 expression *in vivo*

To confirm the regulation of caspase-3 by miR-221, a liver-specific miR-221 transgenic (TG) mouse model (13) was used. Caspase-3 protein levels were quantified by WB analysis in liver samples from 25 TG and 16 wild-type (WT) animals. A 1.4-fold decrease of caspase-3 expression was observed in TG mice with respect to WT controls (Student *t* test: $P = 0.022$; Fig. 6A and B). Moreover, to demonstrate that miR-221 was able to regulate caspase-3 expression *in vivo*, we performed miR-221 silencing in this TG mouse model by means of chemically modified oligonucleotides (13). A mean 2.0-fold increase of caspase-3 protein levels was detected in liver tissue of anti-miR-221-treated mice with respect to the control group (Fig. 6C). Furthermore, we observed that caspase-3 upregulation was maintained in anti-miR-221–treated animals also following sorafenib administration in comparison with vehicle-treated mice. *In vivo* miR-221 silencing was verified in both settings by QPCR analysis (Fig. 6D). These findings proved the caspase-3 targeting by miR-221 *in vivo* and suggested that this molecular mechanism might contribute to sorafenib resistance in miR-221–overexpressing HCCs.

MiR-221 and caspase-3 correlation was also investigated in the tumor tissue from the DEN-induced HCC rat model. As reported in Fig. 1A, when comparing HCC versus its matched surrounding liver tissue, miR-221 expression increased in 65% of HCC tissues, while caspase-3 mRNA and protein levels decreased in 70% and 50% of HCC nodules, respectively. An inverse correlation between miR-221 and caspase-3 was observed at both mRNA and protein levels in rat HCCs (Pearson correlation: $P = 0.009$ and 0.04, respectively; Fig. 6E and F; Supplementary Fig. S3F). We previously demonstrated that miR-221 regulates apoptosis through Bmf targeting (3). Here, we confirm an inverse correlation between miR-221 and Bmf mRNA (Pearson correlation: $R = -0.53$, $P = 0.008$) and a positive correlation between Bmf and caspase-3 mRNA (Pearson correlation: $R = 0.71$, $P < 0.0001$) in rat HCCs, suggesting that miR-221 regulates apoptosis through a multitarget activity (Supplementary Fig. S3G and S3H). *In vitro* experiments confirmed the ability of miR-221 to target contemporaneously caspase-3 and Bmf proteins in transfected HepG2 and SNU449 cells. Moreover, the silencing of caspase-3 slightly decreased Bmf protein levels (Supplementary Fig. S3I), letting us to hypothesize a complex interplay among miR-221 and these two proapoptotic targets.

Finally, we investigated the relationship between miR-221 and caspase-3 levels in 60 patients surgically resected for HCC. An inverse correlation between miR-221 and its target gene is shown in Fig. 6G (Pearson correlation: $R = -0.45$, $P < 0.0001$). In line with the HCC rat model, a mean 3.0-fold increase of miR-221 levels was detected in HCC samples with respect to matched cirrhotic livers, whereas similar miR-221 levels were quantified in normal livers and nontumor samples. In addition, comparable miR-221 levels were observed in HCC patients and HCC cell lines with low basal levels (HepG2, Hep3B, and Huh-7; Supplementary Fig. S3L). As previously reported, high miR-221 levels were associated with HCC multifocality (Student *t* test, $P = 0.013$; Fig. 6H; refs. 3). Here, we also report an association between reduced caspase-3 expression and HCC multifocality (Student *t* test, $P = 0.02$; Fig. 6I). Moreover, we investigated the possible associations between miR-221 and caspase-3 expression and tumor characteristics. No association between miR-221 or caspase-3 mRNA levels and clinicopathologic features (AFP serum levels, tumor size, etiology, and grading) was detected in this cohort of surgically resected patients (Supplementary Fig. S4). These data confirm that miR-221 and caspase-3 aberrant expression in HCC is associated

Published OnlineFirst January 17, 2017; DOI: 10.1158/1078-0432.CCR-16-1464

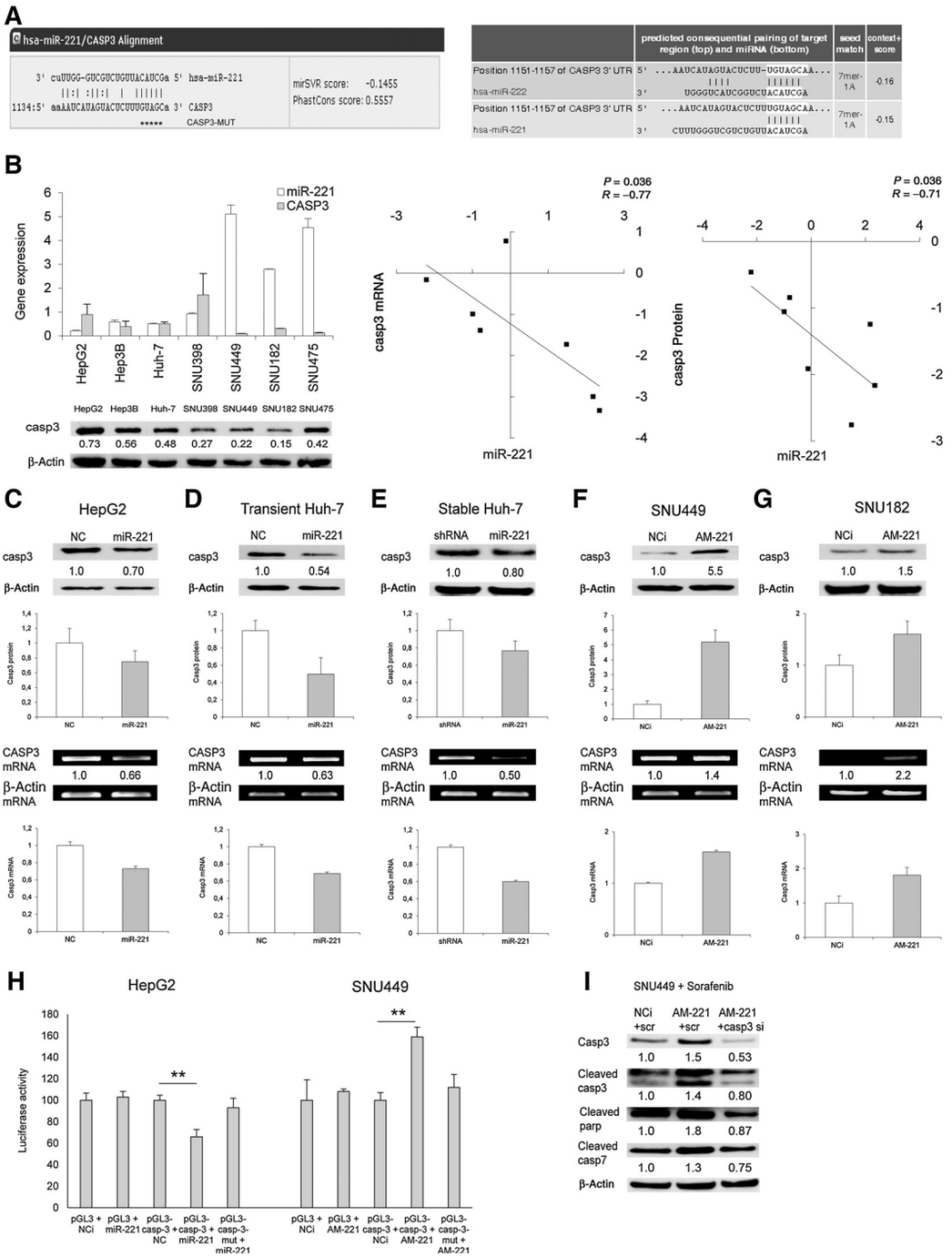

Figure 5.

MiR-221 targets caspase-3 in HCC. **A,** MiR-221 hypothetical binding site in caspase-3 3′UTR as shown by MiRanda and TargetScan algorithms. Stars represent the mutagenized basis in the reporter assay. **B,** QPCR and WB analyses of miR-221 and caspase-3 levels in HCC-derived cell lines. The y-axis reports the $2^{-\Delta\Delta Ct}$ values corresponding to miR-221 or caspase-3 mRNA levels. Correlation graphs represent the relationship between miR-221 and caspase-3 mRNA and protein levels. All the values are in a $\log_2$ form. **C,** Western blot, RT-PCR, and QPCR analyses in miR-221 overexpressing HepG2 cells. **D** and **E,** Western blot, RT-PCR, and QPCR analyses in transient and stable miR-221 overexpressing Huh-7 cells. **F** and **G,** Western blot, RT-PCR and QPCR analyses in miR-221 silenced SNU449 and SNU182 cells. **B–G,** β-actin was used to normalize PCR and WB data. **C–G,** Bar charts below WB images display mean ± SD values relative to immunoblot quantification of three different replicates. Bar charts below RT-PCR images represent mean ± SD values relative to QPCR analysis. **H,** Luciferase reporter assay in HepG2 and SNU449 cells cotransfected with WT or mutated pGL3-casp3 vector and miR-221 or AM-221. **I,** Western blot analysis of apoptotic markers in cotransfected SNU449 cells subjected to sorafenib treatment. β-Actin was used as housekeeping gene. **C–I,** pGL3: empty reporter vector; NC: pre-miR–negative control; NCi: anti-miR–negative control; AM: anti-miR-221; shRNA: scramble short hairpin RNA control vector; scr: scramble oligonucleotides; si: small interfering RNAs.

Published OnlineFirst January 17, 2017; DOI: 10.1158/1078-0432.CCR-16-1464

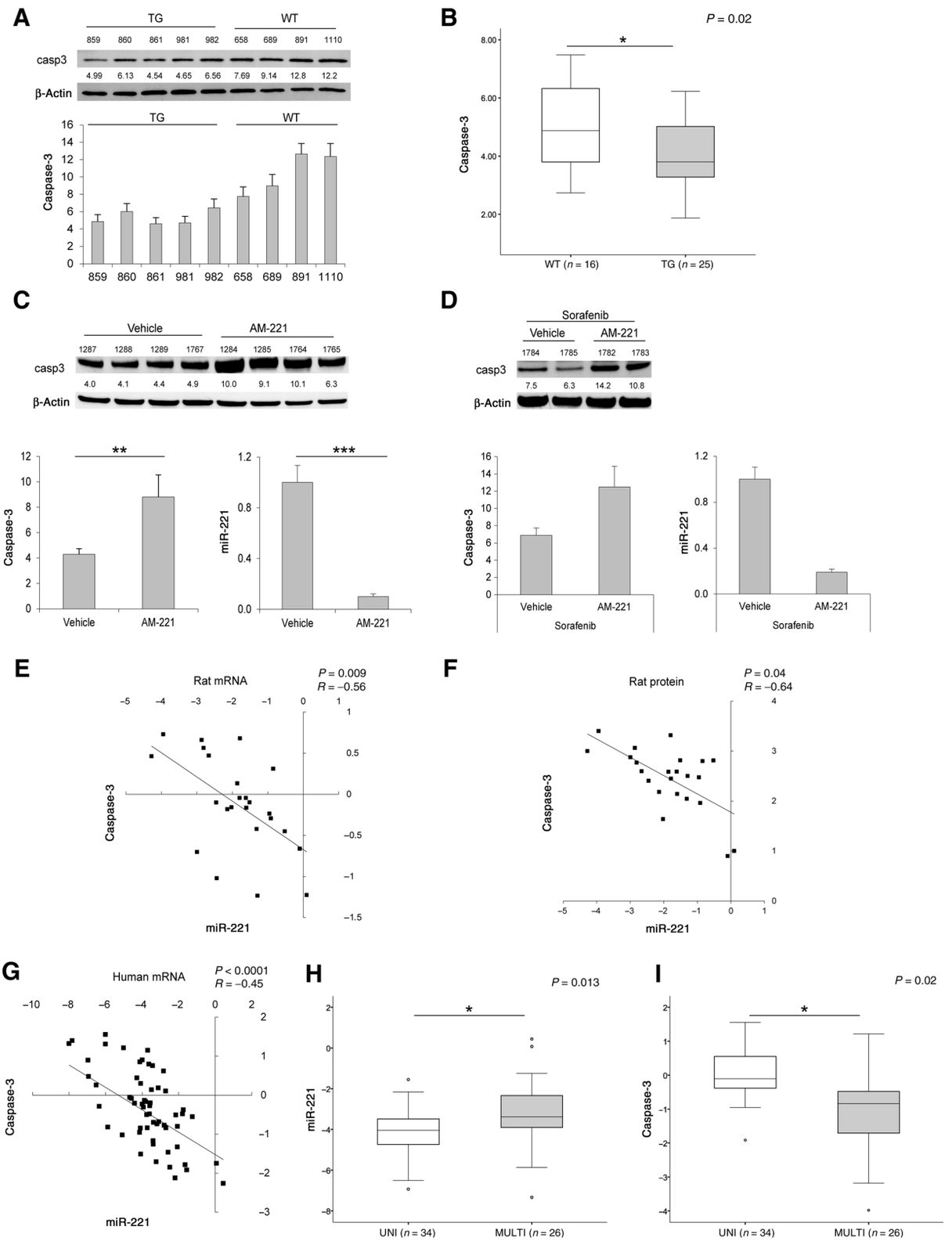

Published OnlineFirst January 17, 2017; DOI: 10.1158/1078-0432.CCR-16-1464

with tumor multinodularity but is independent from other clinical variables.

Discussion

The oncogenic function of miR-221 in hepatocarcinogenesis is well documented (13, 19, 24). Similarly, its role in the regulation of cell proliferation, apoptosis (1, 3, 5), and treatment resistance (14–16) was previously ascertained. In an orthotopic mouse model of HCC, Park demonstrated the therapeutic efficacy of miR-221 inhibition, suggesting miR-221 as a target in patients with HCC (26). These findings were confirmed in our transgenic HCC mouse model, in which anti-miR-221 systemic treatment reduced number and size of HCC nodules (13).

MiRNAs modulation triggered significant effects in the response to anticancer treatments in different cancers. Specifically, miR-221 overexpression in HER-2–positive breast cancer cells inhibited apoptosis and promoted metastasis and trastuzumab resistance by targeting *PTEN*. This study suggested a role of miR-221 as a potential biomarker for the assessment of progression and poor prognosis, as well as a novel target for trastuzumab-combined treatment for HER2-positive breast cancer (27). Similarly, miR-221 silencing sensitized HCC and NSCLC cells to TRAIL by regulating *PTEN* and *TIMP3* (16). A recent study reported miR-221 involvement in dexamethasone resistance through *PUMA* downregulation in multiple myeloma, suggesting miR-221 as a marker of prognosis and clinical response in this context (28). Here, we report miR-221 overexpression in HCC tissue as a molecular event associated with resistance to sorafenib in two HCC animal models. In particular, in the chemically induced HCC rat model an association between high miR-221 intratumor levels and sorafenib resistance was observed, whereas in the xenograft mouse model a direct correlation between miR-221 levels and tumor size was registered. We also demonstrated that caspase-3 is a direct target of miR-221 in HCC, further suggesting miR-221 inhibition as a therapeutic approach aimed to contrast resistance to sorafenib. A recent study describes an inverse correlation between caspase-3 and miR-221 in several cancer cell lines (29), but no clear evidence of a direct targeting was provided. Therefore, to our knowledge, this is the first time that caspase-3 is shown to be directly modulated by miR-221 in HCC. Moreover, here we showed a complex regulatory network between miR-221 and its two proapoptotic targets, caspase-3 and Bmf. Indeed, we confirmed our previous findings (3) reporting a mutual regulation between Bmf and caspase-3 expression and activation in *in vitro* models and we identified a positive correlation between them in preclinical animal models. We might speculate that both targets are important for miR-221 biological activity and that the prevalence of one of them might be dependent on cell context, basal levels, and type of apoptotic stimuli.

A clinical challenge in the oncology field is represented by the identification of non-invasive biomarkers to be used for the prognostic stratification and for the personalization of treatments. Here, we describe an association between miR-221 circulating levels and response to sorafenib in animal models and in patients with advanced HCC undergoing sorafenib treatment. An inverse correlation between miR-221 serum levels (at the end of treatment) and tumor size was detected in treated animals, letting us to hypothesize low miR-221 circulating levels as a possible biomarker of sorafenib resistance. In HCC patients, sorafenib treatment determined an increase of miR-221 circulating levels only in responders. Conversely, before sorafenib start, lower miR-221–circulating levels, assessed at baseline, were associated with response to treatment. Even though the patient cohorts tested here are too small to draw any conclusion, circulating miR-221 might deserve attention as a candidate noninvasive biomarker of response to sorafenib to be tested in prospective trials.

Because sorafenib treatment influences miR-221 intratumoral and circulating levels, we next investigated the mechanisms sustaining miR-221 secretion from neoplastic cells, by exploring the effects of sorafenib in HCC-derived cell lines. Sorafenib administration determined the extrusion of miR-221 from HCC cells into cell culture supernatant in an exosome-dependent manner, determining a reduction of its intracellular levels. Because several proapoptotic factors, such as *BMF*, *BIM*, and *PUMA*, are miR-221 targets (3, 30, 31), the secretion of this oncomiRNA in the extracellular compartment might decrease its intracytoplasmic levels, thus reducing its antiapoptotic activity and sensitizing HCC cells to sorafenib. These events were demonstrated in HCC cells, and we can hypothesize that a similar mechanism might occur in primary tumors, even though we cannot exclude that the tumor surrounding tissue or tumor infiltrating cells can contribute to miR-221 release into the bloodstream. Although we cannot provide a direct demonstration of miR-221 provenience, findings obtained from two animal models, cell lines, and a restricted series of patients with advanced HCC

Figure 6.

MiR-221 targets caspase-3 *in vivo*. **A,** Western blot analysis of caspase-3 expression in miR-221 liver-specific transgenic (TG) and WT mice (representative cases). β-Actin was used as housekeeping gene. Numbers represent the densitometric analysis of WB bands normalized for the housekeeping gene. The bar chart below WB image displays mean ± SD values relative to immunoblot quantification of three different replicates. **B,** Box plot graph of caspase-3 expression in TG and WT mice. The y-axis reports the $2^{-\Delta\Delta Ct}$ values corresponding to caspase-3 expression. **C,** Western blot and QPCR analyses of caspase-3 and miR-221 expression in TG mice treated with anti-miR-221 oligonucleotides (AM-221) or with vehicle (representative cases). **D,** Western blot and QPCR analyses of caspase-3 and miR-221 expression in TG mice treated with anti-miR-221 oligonucleotides (AM-221) or with vehicle and subjected to sorafenib administration. **C** and **D,** β-Actin was used as a housekeeping gene. Numbers represent the densitometric analysis of WB bands normalized for the housekeeping gene. The bar charts below WB images display mean ± SD values of caspase-3 expression in the two mice groups. **E** and **F,** Negative correlation between miR-221 expression and caspase-3 mRNA ($N = 24$) or caspase-3 protein ($N = 23$) levels in the DEN-HCCs. The x and y-axes report the $2^{-\Delta\Delta Ct}$ values corresponding to miR-221 levels and caspase-3 mRNA or protein levels ($\log_2$ form). **G,** Negative correlation between miR-221 expression and caspase-3 mRNA ($N = 60$) levels in human HCCs. The x and y-axes report the $2^{-\Delta\Delta Ct}$ values corresponding to miR-221 and caspase-3 mRNA levels ($\log_2$ form). **H** and **I,** Box plot graph of miR-221 and caspase-3 expression in unifocal (UNI) and multifocal (MULTI) human HCCs. The y-axis reports the $2^{-\Delta\Delta Ct}$ values corresponding to miR-221 or caspase-3 expression ($\log_2$ form). B-actin was used for WB and qPCR normalization.

Published OnlineFirst January 17, 2017; DOI: 10.1158/1078-0432.CCR-16-1464

are consistent with its role as a candidate biomarker of likelihood of response to sorafenib, as well as a noninvasive and dynamic assay to be validated in prospective clinical studies in HCC patients.

Disclosure of Potential Conflicts of Interest

L. Bolondi reports receiving commercial research grants from Bayer, Bristol-Myers Squibb, Daiichi, and Polaris; reports receiving speakers bureau honoraria from Bayer, Bristol-Myers Squibb, Eli-Lilly, Esaote, and Sirtex Bracco; and is a consultant/advisory board member for Bayer, Bristol-Myers Squibb, and Sirtex. No potential conflicts of interest were disclosed by the other authors.

Authors' Contributions

Conception and design: F. Fornari, L. Gramantieri
Development of methodology: F. Fornari, D. Pollutri, C. Patrizi, T. La Bella
Acquisition of data (provided animals, acquired and managed patients, provided facilities, etc.): F. Fornari, S. Marinelli, A.C. Gardini, G. Marisi, M.B. Toaldo, M. Baglioni, V. Salvatore, E. Callegari, M. Baldassarre, M. Galassi, C. Giovannini, M. Cescon, M. Ravaioli, M. Negrini, L. Gramantieri
Analysis and interpretation of data (e.g., statistical analysis, biostatistics, computational analysis): F. Fornari, M. Ravaioli, L. Gramantieri
Writing, review, and/or revision of the manuscript: F. Fornari, V. Salvatore, M. Negrini, L. Gramantieri
Administrative, technical, or material support (i.e., reporting or organizing data, constructing databases): M. Ravaioli
Study supervision: L. Bolondi, L. Gramantieri

Grant Support

This study was supported by Programma di Ricerca Regione-Università 2010-2012, Regione Emilia-Romagna, Bando "Ricerca Innovativa," to L. Bolondi and L.G. "Innovative approaches to the diagnosis and pharmacogenetic-based therapies of primary hepatic tumors, peripheral B and T-cell lymphomas and lymphoblastic leukaemias". Programma di Ricerca Regione-Università 2010-2012, Regione Emilia-Romagna, Bando "Alessandro Liberati," to F. Fornari "Identification of innovative microRNAs-based biomarkers and anticancer strategies for the treatment of Hepatocellular carcinoma." Italian Ministry of University and Research – PRIN 2010-2011 to L. Bolondi Fondazione del Monte in Bologna to L. Gramantieri.

The costs of publication of this article were defrayed in part by the payment of page charges. This article must therefore be hereby marked *advertisement* in accordance with 18 U.S.C. Section 1734 solely to indicate this fact.

Received June 9, 2016; revised November 29, 2016; accepted December 20, 2016; published OnlineFirst January 17, 2017.

References

1. Fornari F, Gramantieri L, Ferracin M, Veronese A, Sabbioni S, Calin GA, et al. MiR-221 controls CDKN1C/p57 and CDKN1B/p27 expression in human hepatocellular carcinoma. Oncogene 2008;27:5651–61.
2. Gramantieri L, Fornari F, Callegari E, Sabbioni S, Lanza G, Croce CM, et al. MicroRNA involvement in hepatocellular carcinoma. J Cell Mol Med 2008;12:2189–204.
3. Gramantieri L, Fornari F, Ferracin M, Veronese A, Sabbioni S, Calin GA, et al. MicroRNA-221 targets Bmf in hepatocellular carcinoma and correlates with tumor multifocality. Clin Cancer Res 2009;15:5073–81.
4. Ciafre SA, Galardi S, Mangiola A, Ferracin M, Liu CG, Sabatino G, et al. Extensive modulation of a set of microRNAs in primary glioblastoma. Biochem Biophys Res Commun 2005;334:1351–58.
5. Zhang CZ, Zhang JX, Zhang AL, Shi ZD, Han L, Jia ZF, et al. MiR-221 and miR-222 target PUMA to induce cell survival in glioblastoma. Mol Cancer 2010;9:229.
6. He H, Jazdzewski K, Li W, Liyanarachchi S, Nagy R, Volinia S, et al. The role of microRNA genes in papillary thyroid carcinoma. Proc Natl Acad Sci U S A 2005;102:19075–80.
7. Pallante P, Visone R, Ferracin M, Ferraro A, Berlingieri MT, Troncone G, et al. MicroRNA deregulation in human thyroid papillary carcinomas. Endocr Relat Cancer 2006;13:497–508.
8. Lee EJ, Gusev Y, Jiang J, Nuovo GJ, Lerner MR, Frankel WL, et al. Expression profiling identifies microRNA signature in pancreatic cancer. Int J Cancer 2007;120:1046–54.
9. Galardi S, Mercatelli N, Giorda E, Massalini S, Frajese GV, Ciafre SA, et al. miR-221 and miR-222 expression affects the proliferation potential of human prostate carcinoma cell lines by targeting p27Kip1. J Biol Chem 2007;282:23716–24.
10. Felicetti F, Errico MC, Bottero L, Segnalini P, Stoppacciaro A, Biffoni M, et al. The promyelocytic leukemia zinc finger-microRNA-221/-222 pathway controls melanoma progression through multiple oncogenic mechanisms. Cancer Res 2008;68:2745–54.
11. Rao X, Di Leva G, Li M, Fang F, Devlin C, Hartman-Frey C, et al. MicroRNA-221/222 confers breast cancer fulvestrant resistance by regulating multiple signaling pathways. Oncogene 2011;30:1082–97.
12. Gottardo F, Liu CG, Ferracin M, Calin GA, Fassan M, Bassi P, et al. Micro-RNA profiling in kidney and bladder cancers. Urol Oncol 2007;25:387–92.
13. Callegari E, Elamin BK, Giannone F, Milazzo M, Altavilla G, Fornari F, et al. Liver tumorigenicity promoted by microRNA-221 in a mouse transgenic model. Hepatology 2012;56:1025–33.
14. Fornari F, Milazzo M, Galassi M, Callegari E, Veronese A, Miyaaki H, et al. p53/mdm2 feedback loop sustains miR-221 expression and dictates the response to anticancer treatments in hepatocellular carcinoma. Mol Cancer Res 2014;12:203–16.
15. Gan R, Yang Y, Yang X, Zhao L, Lu J, Meng QH. Downregulation of miR-221/222 enhances sensitivity of breast cancer cells to tamoxifen through upregulation of TIMP3. Cancer Gene Ther 2014;21:290–96.
16. Garofalo M, Di Leva G, Romano G, Nuovo G, Suh SS, Ngankeu A, et al. miR-221&222 regulate TRAIL resistance and enhance tumorigenicity through PTEN and TIMP3 downregulation. Cancer Cell 2009;16:498–509.
17. Mitchell PS, Parkin RK, Kroh EM, Fritz BR, Wyman SK, Pogosova-Agadjanyan EL, et al. Circulating microRNAs as stable blood-based markers for cancer detection. Proc Natl Acad Sci U S A 2008;105:10513–18.
18. Ferracin M, Lupini L, Salamon I, Saccenti E, Zanzi MV, Rocchi A, et al. Absolute quantification of cell-free microRNAs in cancer patients. Oncotarget 2015;6:14545–55.
19. Gramantieri L, Ferracin M, Fornari F, Veronese A, Sabbioni S, Liu CG, et al. Cyclin G1 is a target of miR-122a, a microRNA frequently downregulated in human hepatocellular carcinoma. Cancer Res 2007;67:6092–99.
20. Edmondson HA, Steiner PE. Primary carcinoma of the liver: a study of 100 cases among 48,900 necropsies. Cancer 1954;7:462–503.
21. Giovannini C, Minguzzi M, Baglioni M, Fornari F, Giannone F, Ravaioli M, et al. Suppression of p53 by Notch3 is mediated by Cyclin G1 and sustained by MDM2 and miR-221 axis in hepatocellular carcinoma. Oncotarget 2014;5:10607–20.
22. Fornari F, Gramantieri L, Giovannini C, Veronese A, Ferracin M, Sabbioni S, et al. MiR-122/cyclin G1 interaction modulates p53 activity and affects doxorubicin sensitivity of human hepatocarcinoma cells. Cancer Res 2009;69:5761–67.
23. Fornari F, Ferracin M, Trere D, Milazzo M, Marinelli S, Galassi M, et al. Circulating microRNAs, miR-939, miR-595, miR-519d and miR-494, Identify Cirrhotic Patients with HCC. PLoS One 2015;10:e0141448.
24. Pineau P, Volinia S, McJunkin K, Marchio A, Battiston C, Terris B, et al. miR-221 overexpression contributes to liver tumorigenesis. Proc Natl Acad Sci U S A 2010;107:264–69.
25. Baron Toaldo M, Salvatore V, Marinelli S, Palama C, Milazzo M, Croci L, et al. Use of VEGFR-2 targeted ultrasound contrast agent for the early evaluation of response to sorafenib in a mouse model of hepatocellular carcinoma. Mol Imaging Biol 2015;17:29–37.
26. Park JK, Kogure T, Nuovo GJ, Jiang J, He L, Kim JH, et al. miR-221 silencing blocks hepatocellular carcinoma and promotes survival. Cancer Res 2011;71:7608–16.

27. Ye X, Bai W, Zhu H, Zhang X, Chen Y, Wang L, et al. MiR-221 promotes trastuzumab-resistance and metastasis in HER2-positive breast cancers by targeting PTEN. BMB Rep 2014;47:268–73.
28. Zhao JJ, Chu ZB, Hu Y, Lin J, Wang Z, Jiang M, et al. Targeting the miR-221–222/PUMA/BAK/BAX pathway abrogates dexamethasone resistance in multiple myeloma. Cancer Res 2015;75:4384–97.
29. Ergun S, Arman K, Temiz E, Bozgeyik I, Yumrutas O Safdar M, et al. Expression patterns of miR-221 and its target Caspase-3 in different cancer cell lines. Mol Biol Rep 2014;41: 5877–81.
30. Sharma AD, Narain N, Handel EM, Iken M, Singhal N, Cathomen T, et al. MicroRNA-221 regulates FAS-induced fulminant liver failure. Hepatology 2011;53:1651–61.
31. Terasawa K, Ichimura A, Sato F, Shimizu K, Tsujimoto G. Sustained activation of ERK1/2 by NGF induces microRNA-221 and 222 in PC12 cells. FEBS J 2009;276:3269–76.

Published OnlineFirst January 17, 2017; DOI: 10.1158/1078-0432.CCR-16-1464

Clinical Cancer Research

In Hepatocellular Carcinoma miR-221 Modulates Sorafenib Resistance through Inhibition of Caspase-3–Mediated Apoptosis

Francesca Fornari, Daniela Pollutri, Clarissa Patrizi, et al.

Clin Cancer Res 2017;23:3953-3965. Published OnlineFirst January 17, 2017.